

# Polymeric ionic liquid membranes as electrolytes for lithium battery applications

Mingtao Li · Siming Dong · Shaohua Fang ·  
Li Yang · Shin-ichi Hirano · Jiayang Hu ·  
Xinming Huang

Received: 11 April 2012 / Accepted: 4 July 2012 / Published online: 17 August 2012  
© Springer Science+Business Media B.V. 2012

**Abstract** A new kind of polymeric ionic liquid (PIL) membrane based on guanidinium ionic liquid (IL) with ester and alkyl groups was synthesized. On addition of guanidinium IL, lithium salt, and nano silica in the PIL, a gel PIL electrolyte was prepared. The chemical structure of the PIL and the properties of gel electrolytes were characterized. The ionic conductivity of the gel electrolyte was  $5.07 \times 10^{-6}$  and  $1.92 \times 10^{-4} \text{ S cm}^{-1}$  at 30 and 80 °C, respectively. The gel electrolyte had a low glass transition temperature ( $T_g$ ) under  $-60$  °C and a high decomposition temperature of 310 °C. When the gel polymer electrolyte was used in the Li/LiFePO<sub>4</sub> cell, the cell delivered 142 mAh g<sup>-1</sup> after 40 cycles at the current rates of 0.1 C and 80 °C.

**Keywords** Polymeric ionic liquids · Guanidinium ionic liquids · Polymer electrolytes · Lithium batteries

## 1 Introduction

Ionic liquids (ILs) have emerged as a kind of promising electrolyte due to their unique properties such as negligible

vapor pressure, flame retardancy, thermal stability, and high ionic conductivity [1–4]. They may help reduce or prevent potential safety hazards caused by the exothermic reaction of a typical electrolyte consisting of volatile organic solvents. One of the approaches, utilized ILs as electrolytes, is switching to IL-based polymer membranes by polymerization of the IL monomer or incorporation of the ILs into a certain polymer matrix to form gel polymer electrolytes. Since the viscoelastic nature of polymer electrolytes provides a leak-proof system compared with liquid electrolyte, the electrolytes based on IL-based polymer membranes become one of the most promising candidates for future application in electrochemical devices including lithium batteries, fuel cells, and solar cells [5–8].

Ohno et al. reported various polymeric ionic liquid (PIL) systems such as polycation, polyanion, blend, zwitterionic, and copolymer types [9–12]. Although the physical and chemical properties of the PILs were investigated, very few PILs as electrolytes have been applied in lithium batteries due to their poor compatibility with the interface of electrodes. Recently, a ternary PIL electrolyte containing pyrrolidinium-based ILs was prepared, and the battery performance with the electrolyte was determined [13]. In the paper, the author observed that an addition of ILs in PIL-based electrolytes could improve the interface compatibility between the electrolytes and electrodes, which pointed out a direction for PIL electrolytes in application to lithium batteries.

Guanidinium ILs show exceptional physicochemical properties and have become an intriguing domain of recent research [14–16]. Recently, our group has synthesized a series of new guanidinium IL electrolytes [17, 18] and PIL electrolytes based on guanidinium cations with alkyl groups [19–21]. The electrolytes have been used successfully in lithium batteries at room or elevated temperature.

M. Li · J. Hu · X. Huang  
Department of Chemical Engineering, State Key Laboratory of Multiphase Flow in Power Engineering, Xi'an Jiaotong University, Xi'an Shaanxi 710049, China

S. Dong · S. Fang · L. Yang  
School of Chemistry and Chemical Technology,  
Shanghai Jiaotong University, Shanghai 200240, China

S. Fang · L. Yang (✉) · S. Hirano  
Hirano Institute for Materials Innovation,  
Shanghai Jiaotong University, Shanghai 200240, China  
e-mail: liyangce@sjtu.edu.cn

In the present study, a functional group, the ester group, was introduced in guanidinium cations and a new PIL electrolyte based on the guanidinium cations was synthesized. On addition of guanidinium IL, a gel PIL electrolyte was prepared. Furthermore, nano silica was also added in the electrolytes to increase the mechanical strength of the electrolyte membrane. The gel polymer electrolyte was used in Li/LiFePO<sub>4</sub> cells and showed good performances at the current rates of 0.1 C and 80 °C.

## 2 Experimental

### 2.1 Materials

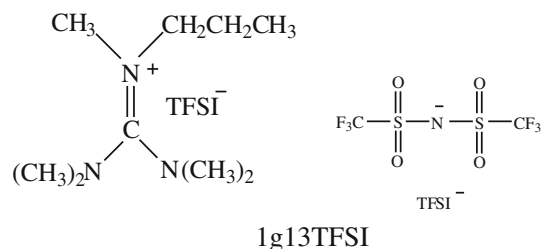
Tetramethylurea, oxalyl chloride, triethylamine, allyl amine, methyl bromoacetate, and methyl acrylate were purchased from Alfa Aesar. Lithium bis(trifluoromethylsulfonyl)imide (LiTFSI) was kindly provided by Morita Chemical Industries Co., Ltd. Nano silicon dioxide (99.8 %, BET 120 m<sup>2</sup> g<sup>-1</sup>, 7–40 nm) was purchased from Aladdin Reagent Inc. All the other chemicals used in the work were of A.R. grade.

### 2.2 Preparation of IL and PIL membrane

An IL, 1g13TFSI, the structure of which is shown in Scheme 1, was prepared by our previous reported methods [22–24]. 2-allyl-1,1,3,3-tetramethylguanidine (1gE) was prepared according to the following methods. 0.1 mol (15.5 g) of the guanidine and 0.13 mol (19.9 g) of methyl bromoacetate (Alfa Aesar, 98+ % purity) were added into 20 ml of acetonitrile for 24 h at 70 °C. The product was washed with ethyl ether and dried thoroughly in vacuum at 50 °C for 24 h to remove the solvent.

1gE–MA–Br is prepared according to the methods illustrated in Scheme 2. The structures of 1gE and 1gE–MA–Br were confirmed using <sup>1</sup>H NMR (Avance III 400). The characterization data are as follows.

1gE: <sup>1</sup>H NMR (400 MHz, CDCl<sub>3</sub>), δ (ppm): 6.03–5.89 (m, 1H), 5.39–5.31 (m, 2H), 4.25–4.00 (m, 2H), 3.84–3.70 (s, 3H), 3.30–3.11 (s, 12H), 3.11–2.99 (s, 2H).



**Scheme 1** The structure of the IL, 1g13TFSI

1gE–MA–Br: <sup>1</sup>H NMR (400 MHz, Acetone-D<sub>6</sub>), δ (ppm): 3.76–3.72 (s, 2H), 3.72–3.57 (s, 6H), 3.20–3.03 (m, 2H), 2.90–2.71 (s, 12H), 2.48–2.28 (m, 1H), 1.99–1.83 (m, 1H), 1.79–1.66 (m, 2H), 1.38–1.22 (d, 2H). *M<sub>n</sub>* = 53,034, *M<sub>w</sub>*/*M<sub>n</sub>* = 2.169, (GPC, polystyrene).

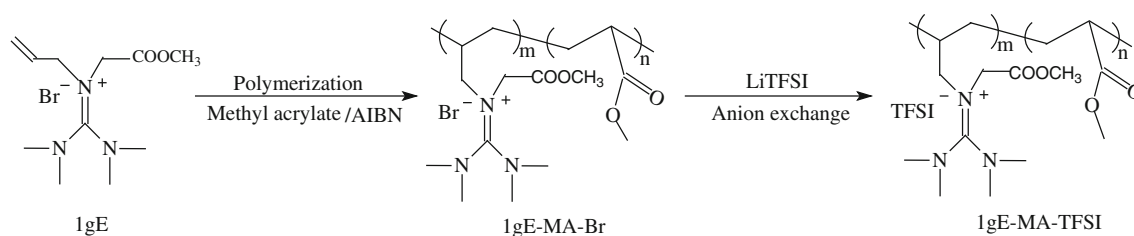
The PIL membrane with TFSI<sup>-</sup> anion, 1gE–MA–TFSI, was obtained by a simple ion-exchange method. 1gE–MA–TFSI and LiTFSI were dissolved in acetone and then stirred at 40 °C for 3 h. The proportion of lithium salt is variable, from 15 to 60 % weight percent based on the amount of the PIL. The transparent polymer membrane was prepared by casting the solution onto Teflon slides, and the membrane was subsequently dried at 80 °C under vacuum for 24 h before conductivity measurement. Anal. Calcd. for 1gE–MA–TFSI: C 48.06, N 1.56, S 3.00. Found: C 47.8; N 1.56; S 3.17.

### 2.3 Preparation of gel polymer electrolyte

1gE–MA–TFSI (0.6 g), LiTFSI (0.12 g), 1g13TFSI (0.3 g), SiO<sub>2</sub> (0.06 g), and acetone (6 ml) were mixed and stirred for 2 h at 40 °C. The mixture was cast onto Teflon slides and then dried in an argon-filled glove box ([O<sub>2</sub>] < 1 ppm, [H<sub>2</sub>O] < 1 ppm) for 48 h.

### 2.4 Characterization and measurement

Structures of the synthesized IL and PIL were confirmed using <sup>1</sup>H NMR, and tetramethylsilane was used as an internal reference for the analysis. The ATR-FT IR spectroscopic measurements were performed on a Perkin-Elmer Spectrum 100 FT IR spectrometer. Differential scanning calorimetry (DSC) was carried out on a Perkin-Elmer Pyris 1 instrument. The measurements were conducted with the temperature range from –60 to 200 °C at a scan rate of 10 °C min<sup>-1</sup> under a continuous nitrogen purge (50 mL min<sup>-1</sup>). Thermogravimetric (TG) measurements of the polymers were conducted on a Perkin-Elmer thermogravimetric analyzer from room temperature to 400 °C at a heating rate of 10 °C min<sup>-1</sup> under a continuous nitrogen purge (50 mL min<sup>-1</sup>). Molecule weights of the polymers were estimated by waters gel permeation chromatography (GPC) using 12 monodisperse polystyrenes (molecular weight range 10<sup>2</sup>–10<sup>7</sup>) as calibration standards. The sample solutions were prepared in *N,N*-dimethylformamide (ca. 3–5 mg mL<sup>-1</sup>) and filtered through 0.45 μm poly(tetrafluoroethylene) syringe-type filters before being injected into the GPC system. The elemental composition (C, N, and S) was measured using an elemental analyzer (Perkin-Elmer 2400II). The ionic conductivity (σ) was determined by means of the complex impedance measurements using a CHI660D Electrochemical Workstation functioning with



**Scheme 2** Illustration for the preparation of PILs, therein  $m = 14.8$ ,  $n = 541.3$

an oscillating voltage of 5 mV from  $10^5$  to 1 Hz frequency range at various temperatures. The polymer membranes were sandwiched between two blocking electrodes. The ionic conductivity was given by

$$\sigma = \frac{L}{RS} \quad (1)$$

where  $R$  is the bulk resistance value which can be estimated from the impedance diagram,  $L$  is the thickness of the polymer membrane, and  $S$  is the area of the blocking electrode.

The electrochemical stability of the gel polymer electrolyte was measured on a CHI660D Electrochemical Workstation by means of linear sweep voltammetry (LSV) using the cell Li/gel polymer electrolyte/stainless steel. The scanning rate is  $1 \text{ mV s}^{-1}$ . The cell was assembled and sealed in the glove box. The stainless steel was used as a working electrode. The lithium was used as both reference and counter electrodes.

## 2.5 Cell assembly and instrumentation

Li/LiFePO<sub>4</sub> coin cell was assembled to evaluate the cycle performance of the gel polymer electrolyte in lithium battery applications. The polymer electrolyte membrane was sandwiched between a Li metal anode and a LiFePO<sub>4</sub> cathode. The cathode was prepared by spreading the mixture of LiFePO<sub>4</sub>, acetylene black, and PVdF (dissolved in *N*-methyl-2-pyrrolidone initially) with a weight ratio of 8:1:1 on an Al current collector and then dried at  $110^\circ\text{C}$  under vacuum for 24 h to remove the solvent. The loading of active material (LiFePO<sub>4</sub>) was about ca.  $0.90\text{--}1.51 \text{ mg cm}^{-2}$ . Cell assembly was implemented in the argon-filled glove box. All the components in the cells were firstly dried under vacuum and were then put into the glove box. The cells were sealed and then thermally equilibrated in the thermostat chamber at the selected operating temperature ( $80^\circ\text{C}$ ) for 24 h before performance tests. The cell tests were performed by the galvanostatic charge–discharge (C–D) cycling test during 2–4 V using a CT-3,008 W battery testing system (Neware Technology Ltd.) at  $80^\circ\text{C}$ . The current rate was determined by setting the nominal capacity as  $150 \text{ mAh g}^{-1}$  for Li/LiFePO<sub>4</sub> cell.

## 3 Results and discussion

### 3.1 Characterization of IL and PILs

The PILs used in this study were prepared by two steps as illustrated in Scheme 2. The monomer structure of 1gE was characterized by  $^1\text{H}$  NMR, which is shown and assigned in Fig. 1.

The obtained PILs were characterized by ATR-FT IR spectroscopy as indicated in Fig. 2. In Fig. 2, the peaks at  $1,725$  and  $1,155 \text{ cm}^{-1}$  are assigned, respectively, to the C=O and C–O stretching vibration from the ester group of the guanidinium blocks and the methacrylate blocks. The peaks at  $1,445$  and  $1,355 \text{ cm}^{-1}$  are assigned, respectively, to the CH<sub>2</sub> wagging and scissoring from the main polymer chain. The peaks at  $1,607$  and  $1,555 \text{ cm}^{-1}$  are assigned to the C=N and C–N stretching of the guanidinium blocks, respectively. The band at  $3,408 \text{ cm}^{-1}$  corresponding to the bromide group can be observed on the spectra of 1gE–MA–Br, while it disappeared on that of 1gE–MA–TFSI. Instead, the peaks at  $1,347$ ,  $1,183$ ,  $1,134$ ,  $1,052$ , and  $746 \text{ cm}^{-1}$  on the spectra of 1gE–MA–TFSI indicate the existence of the TFSI<sup>−</sup> anions [25, 26]. From the ATR-FT

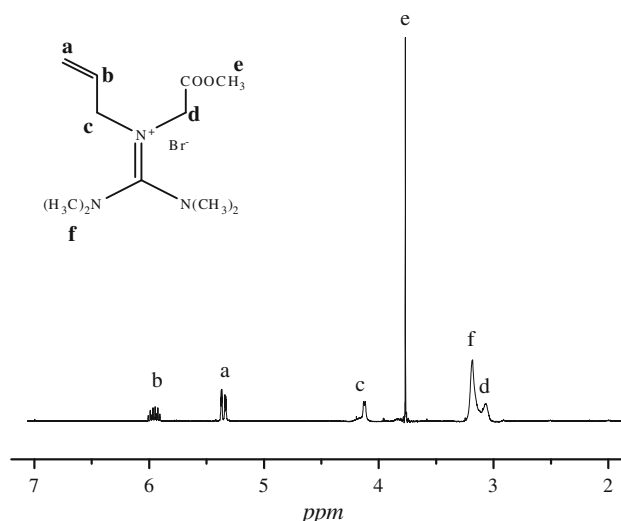


**Fig. 1**  $^1\text{H}$  NMR spectra of 1gE

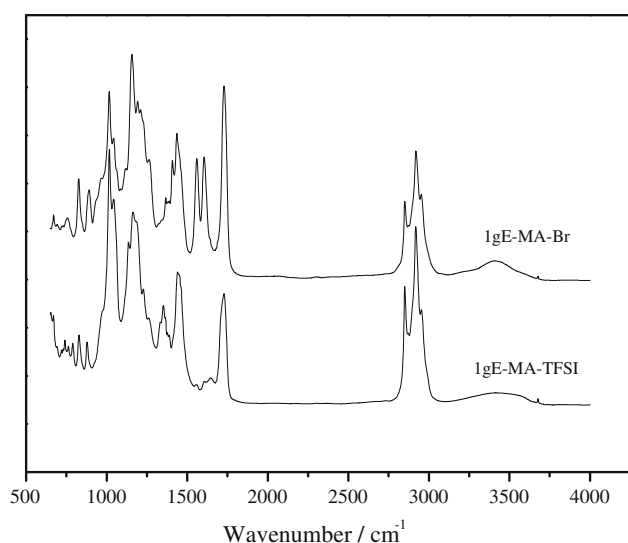


**Fig. 2** ATR-FT IR spectra of PILs, 1gE-MA-Br, and 1gE-MA-TFSI

IR results, we know that the product has the expected chemical structure.

### 3.2 Thermal properties of PILs and gel polymer electrolyte

Thermal properties of the PILs and gel polymer electrolyte were then characterized by DSC and thermogravimetric analysis (TGA) shown in Figs. 3 and 4, respectively.  $T_g$  of PIL with TFSI<sup>−</sup> or bromide anions was about 10 °C, while  $T_g$  of the gel polymer electrolyte was below −60 °C. Herein, the existence of TFSI<sup>−</sup> anions did not bring a slump of  $T_g$ , which is different from our previous report [19]. It is possible that the introduction of the ester group in the guanidinium blocks has changed the local segmental

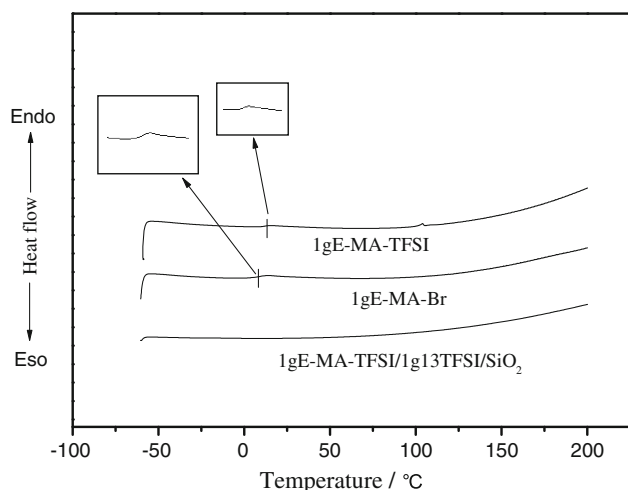


**Fig. 3** DSC curves of the PILs with different anions and gel polymer electrolyte

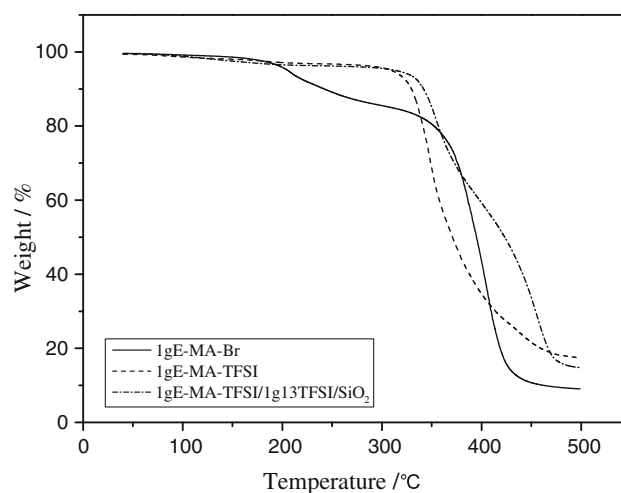


**Fig. 4** TGA profiles of the PILs with different anions and the gel polymer electrolyte

motion of polymer electrolyte. In the gel polymer electrolyte, with the addition of 1g13TFSI,  $T_g$  of the electrolyte sample decreased drastically. This decrease in  $T_g$  may be attributed to 1g13TFSI serving as a plasticizer in the electrolyte sample, which promotes the distancing of the PIL chains and changes the crystalline structure leading to a considerable increase of amorphous phase, as already observed by Pawlicka et al. [27] and our previous report [20]. The TG results are shown in Fig. 4. It is obvious that the PILs with different anions showed different thermal behaviors. 1gE-MA-Br decomposed in two steps in a relatively low temperature, while 1gE-MA-TFSI and the gel polymer electrolyte decomposed at 310 °C exhibiting a better thermal stability.

### 3.3 Effect of the lithium salt concentration in PIL on the ionic conductivity

To determine the optimized composition of the gel polymer electrolyte, the effect of the lithium salt concentration on the ionic conductivity was investigated. 1gE-MA-TFSI was mixed with LiTFSI at different ratios. The composition is shown as PIL + wt% salt, where wt% can be given by

$$\text{wt \%} = \frac{W_{\text{salt}}}{W_{\text{PIL}}} \times 100 \% \quad (2)$$

where  $W_{\text{salt}}$  and  $W_{\text{PIL}}$  denote, respectively, the weight of lithium salt and the host PIL.

The temperature dependence of ionic conductivity is shown in Fig. 5. All the samples show a linear increase of ionic conductivity with temperature, which obeys the Arrhenius equation, Eq. (3):

$$\sigma(T) = A \cdot \exp\left(\frac{-E_a}{RT}\right) \quad (3)$$

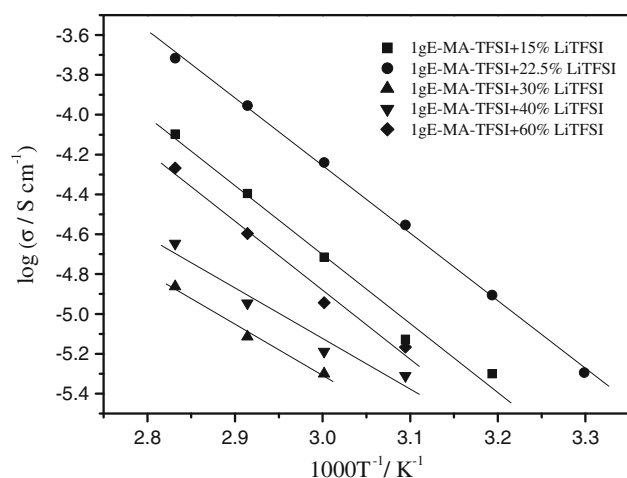


**Fig. 5** Temperature dependence of ionic conductivity for 1gE-MA-TFSI with different lithium salt concentration (15, 22.5, 30, 40, and 60 %). Note The data of 1gE-MA-TFSI + 30, 40, and 60 wt% LiTFSI at near room temperature were deleted because impedances exceeded the measurement range of the electrochemical workstation

where  $A$  is the pre-exponential factor,  $E_a$  is the activation energy for ionic conductivity, and  $T$  is the absolute temperature value. In the gel polymer electrolyte system, the change of conductivity with temperature may be due to the segmental motion of the polymer chains leading to an increase in free volume in the system, which will provide an easy pathway for the transitional motion of the ions. The segmental motion also permits the ions to hop from one site to another. As the temperature increases, both the segmental motion and transitional ionic motion in the system will increase due to the high activation energy and it will improve the ionic conductivity [13].

It can be observed from the figure that 1gE-MA-TFSI + 22.5 wt% LiTFSI has the highest ionic conductivity and the corresponding maximum values of the ionic conductivity are  $5.07 \times 10^{-6} \text{ S cm}^{-1}$  at  $30^\circ\text{C}$  and  $1.92 \times 10^{-4} \text{ S cm}^{-1}$  at  $80^\circ\text{C}$ . The increase of ionic conductivity with the addition of lithium salts at a low concentration was owing to the increased number of charge carriers dissociated by lithium salts. At a higher concentration, the conductivity decreased because the lithium salts aggregated and formed crystalline phases or charged triplets which resulted in a decreased number of mobile charge carriers and lower mobility [28]. As a result, 20 wt% LiTFSI was selected as the optimized lithium salt concentration in the gel polymer electrolyte.

### 3.4 Electrochemical stability

The electrochemical stability of the 1gE-MA-TFSI/1g13TFSI/SiO<sub>2</sub> gel polymer electrolyte was measured by LSV as shown in Fig. 6. The anodic limiting potential of

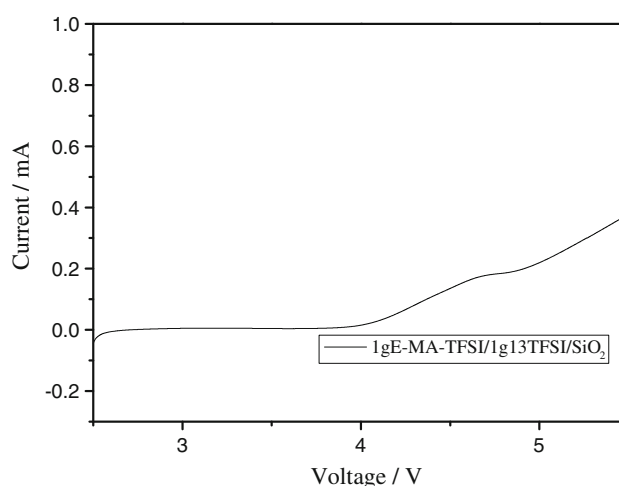


**Fig. 6** Linear sweep voltammograms of 1gE-MA-TFSI/1g13TFSI/SiO<sub>2</sub> gel polymer electrolyte (Li/gel polymer electrolyte/SS cell,  $1 \text{ mV s}^{-1}$ , 2–7 V,  $80^\circ\text{C}$ )

electrolyte is about 4.2 V versus Li/Li<sup>+</sup>, which means the electrolyte is suitable to be applied in lithium batteries.

### 3.5 Charge–discharge characteristics of Li/LiFePO<sub>4</sub> cells

The charge–discharge characteristics of Li/LiFePO<sub>4</sub> cells using the gel polymer electrolyte were investigated at the current rates of 0.1 C and  $80^\circ\text{C}$ . The composition of gel polymer electrolyte was arranged for 1gE-MA-TFSI + 20 wt% LiTFSI + 50 wt% 1g13TFSI + 10 wt% SiO<sub>2</sub>, which referenced our previous research [20]. 10 wt% SiO<sub>2</sub> added in the gel polymer electrolytes was to increase the mechanical strength of the electrolyte membrane. Figure 7 shows the cycle numbers dependence of the charge–discharge capacity and coulombic efficiency of the cell.

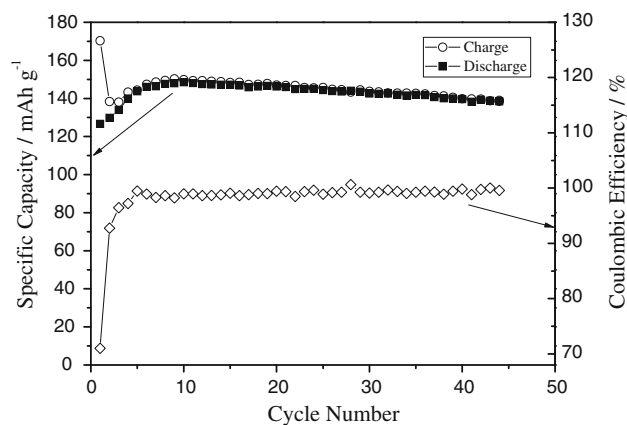


**Fig. 7** The cycle numbers dependence of the charge–discharge capacity and coulombic efficiency of Li/LiFePO<sub>4</sub> cells with 1gE-MA-TFSI/1g13TFSI/SiO<sub>2</sub> gel polymer electrolytes. (Charge–discharge current rate is 0.1 C,  $80^\circ\text{C}$ )



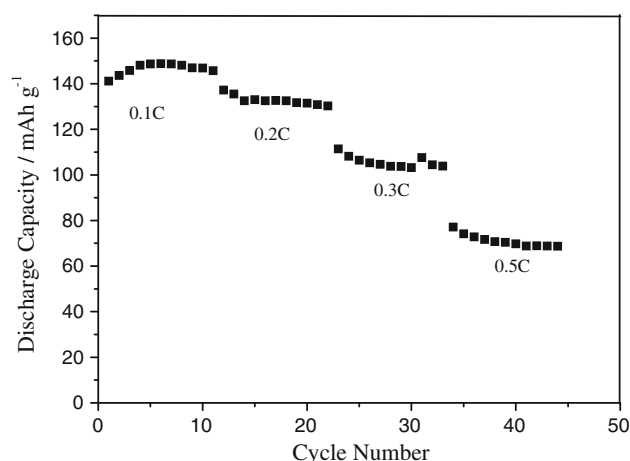


**Fig. 8** Discharge capacity of Li/LiFePO<sub>4</sub> cells with 1gE-MA-TFSI/1g13TFSI/SiO<sub>2</sub> gel polymer electrolyte at different current rates. (Charge current rate is 0.1 C; discharge current rates range from 0.1 to 0.5 C, 80 °C)

The cell presented an initial discharge capacity of 127 mAh g<sup>-1</sup>. It soon increased to 148 mAh g<sup>-1</sup> at the 10th cycle. The cell exhibited a good performance and its discharge capacity was about 142 mAh g<sup>-1</sup> at the 40th cycle. After the initial 4 cycles, the coulombic efficiency was higher than 98 %, which showed the excellent reversibility of the cell. The increase of specific capacity and coulombic efficiency in initial cycles of the cell indicated that the SEI film was formed on the interface of electrodes with the electrolyte or the IL was redistributed inside the gel polymer electrolyte during the process [29].

The discharge capacity at different discharge current rates is shown in Fig. 8. The discharge capacity decreased with the increase of discharge current rates. The fall of discharge capacity at elevated current rates is associated with the low lithium ion transference number of the IL-based polymer electrolyte [30]. Since the performance at a higher current rate could be improved by the addition of other additives, a further study is in progress to overcome this difficulty.

#### 4 Conclusions

A new kind of PIL membrane based on guanidinium IL with ester and alkyl groups was synthesized. Incorporating the guanidinium IL, lithium salt, and nano silica in the PIL host, a gel electrolyte was prepared. The chemical structures and properties of the PIL and gel polymer electrolyte, respectively, were characterized. It should be noted that the gel polymer electrolyte, 1gE-MA-TFSI/1g13TFSI/SiO<sub>2</sub>, showed exceptional electrochemical properties. It was used in Li/LiFePO<sub>4</sub> cells without any additives and exhibited good performance at the current rates of 0.1 C and 80 °C.

**Acknowledgments** The authors thank the Research Center of Analysis and Measurement of Shanghai Jiao Tong University for help in the elemental analysis. We are grateful for financial support for this work from the National Natural Science Foundation of China (Grants No. 21103108 and 21173148) and the Postdoctoral Foundation of China (Grants No. 2012M511991).

#### References

1. Marsh KN, Boxall JA, Lichtenthaler R (2004) *Fluid Phase Equilib* 219:93
2. Davis JH (2004) *Chem Lett* 33:1072
3. Hagiwara R, Ito Y (2000) *J Fluor Chem* 105:221
4. Armand M, Endres F, MacFarlane DR, Ohno H, Scrosati B (2009) *Nat Mater* 8:621
5. Ohno H (2007) *Macromol Symp* 249:551
6. Qin D, Guo XZ, Sun HC, Luo YH, Meng QB, Li DM (2011) *Prog Chem* 23:557
7. Hagiwara R, Lee JS (2007) *Electrochemistry* 75:23
8. Deligoz H, Yilmazoglu M (2011) *J Power Sources* 196:3496
9. Ogihara W, Washiro S, Nakajima H, Ohno H (2006) *Electrochim Acta* 51:2614
10. Ogihara W, Kosukegawa H, Ohno H (2006) *Chem Commun* 3637
11. Ohno H, Washiro S, Yoshizawa M (2004) *Abstr Pap Am Chem Soc* 227:U461
12. Yoshizawa M, Ogihara W, Ohno H (2002) *Polym Advan Technol* 13:589
13. Appetecchi GB, Kim GT, Montanino M, Carewska M, Marcilla R, Mecerreyes D, De Meazza I (2010) *J Power Sources* 195:3668
14. Sairi NA, Yusoff R, Alias Y, Aroua MK (2011) *Fluid Phase Equilib* 300:89
15. Yu Z, Gorlov M, Boschloo G, Kloo L (2010) *J Phys Chem C* 114:22330
16. Li DM, Wang MY, Wu JF, Zhang QX, Luo YH, Yu ZX, Meng QB, Wu ZJ (2009) *Langmuir* 25:4808
17. Fang SH, Yang L, Wang JX, Zhang HQ, Tachibana K, Kamijima K (2009) *J Power Sources* 191:619
18. Fang SH, Yang L, Wei C, Jiang C, Tachibana K, Kamijima K (2009) *Electrochim Acta* 54:1752
19. Li M, Yang L, Fang S, Dong S (2011) *J Memb Sci* 366:245
20. Li M, Yang L, Fang S, Dong S, Hirano S-i, Tachibana K (2011) *J Power Sources* 196:8662
21. Li M, Yang L, Fang S, Dong S, Hirano S-i, Tachibana K (2012) *Polym Int* (in press)
22. Gao Y, Arritt SW, Twamley B, Shreeve JM (2005) *Inorg Chem* 44:1704
23. Wang P, Zakeeruddin SM, Gratzel M, Kantelehner W, Mezger J, Stoyanov EV, Scherr O (2004) *Appl Phys A Mater* 79:73
24. Xie HB, Zhang SB, Duan HF (2004) *Tetrahedron Lett* 45:2013
25. Pont AL, Marcilla R, De Meazza I, Grande H, Mecerreyes D (2009) *J Power Sources* 188:558
26. Umebayashi Y, Mitsugi T, Fukuda S, Fujimori T, Fujii K, Kanzaki R, Takeuchi M, Ishiguro SI (2007) *J Phys Chem B* 111:13028
27. Pawlicka A, Danczuk M, Wiczeorek W, Zygałło-Monikowska E (2008) *J Phys Chem A* 112:8888
28. Yang Y, Zhang J, Zhou C, Wu S, Xu S, Liu W, Han H, Chen B, Zhao XZ (2008) *J Phys Chem B* 112:6594
29. Shin JH, Henderson WA, Scaccia S, Prosini PP, Passerini S (2006) *J Power Sources* 156:560
30. Ye H, Huang J, Xu JJ, Khalfan A, Greenbaum SG (2007) *J Electrochem Soc* 154:A1048